



Isolation, genetic characterization, and pathogenicity of the porcine epidemic diarrhea virus S-INDEL strain EJS6 in China

Yiye Zhang^{1,2}, Jiahui Guo^{1,2}, Qi Yang^{1,2}, Tong Zhuang^{1,2}, Shaobo Xiao^{1,2} and Liurong Fang^{1,2*} 

Abstract

Porcine epidemic diarrhea virus (PEDV) is a highly infectious intestinal coronavirus that poses a significant threat to the pig industry because of its strong virulence and propensity for mutation and recombination. PEDV is classified into three major genotypes based on the spike (S) gene sequence: G1 (classical), G2 (variant), and S-INDEL (characterized by nucleotide insertions/deletions in the S gene). Both the G1 and G2 genotypes have been frequently detected in China, whereas the S-INDEL strain has rarely been reported or isolated. In this study, we isolated a PEDV S-INDEL strain, designated EJS6, from a pig farm experiencing severe diarrhea in Jiangsu Province, China. Genetic evolution analysis revealed that the Chinese S-INDEL strains represented by EJS6 presented sequence differences from other S-INDEL strains isolated in Europe and the United States, forming a new branch within the S-INDEL genotype. Compared with the G2 strain EHUB4, EJS6 presented a lower viral titer, smaller plaque size, and reduced syncytium-forming ability in Vero cells. We also compared the pathogenicity of EJS6 and EHUB4 in 5-day-old suckling piglets. Both strains exhibited similar levels of fecal virus shedding in the infected piglets; however, the histopathological and mortality results indicated that the pathogenicity of the EJS6 strain was weaker than that of the EHUB4 strain. In summary, we successfully isolated the first Chinese PEDV S-INDEL strain and characterized its genetic evolution and pathogenicity, thereby enhancing our understanding of the prevalence of PEDV in China.

Keywords Porcine epidemic diarrhea virus, S-INDEL strain, Genetic characterization, Evolution, Pathogenicity

Introduction

Porcine epidemic diarrhea virus (PEDV), a member of the *Alphacoronavirus*, within the family *Coronaviridae*, causes diarrhea, vomiting, anorexia, dehydration, and death in piglets (Have et al. 1992). Although pigs of all ages can be infected and exhibit varying degrees of

symptoms, the condition is particularly severe in suckling piglets, with a mortality rate reaching 100% (Chen et al. 2011). PEDV is an enveloped, single-stranded positive-sense RNA virus with a full-length genome of approximately 28 kb. The genome comprises seven open reading frames (ORFs) organized in the order ORF1a, ORF1ab, spike (S) glycoprotein gene, ORF3 accessory protein-encoding gene, envelope (E) gene, membrane (M) gene, and nucleocapsid (N) gene (Song and Park 2012). Like other coronaviruses, the S protein of PEDV is heavily glycosylated and plays a crucial role in virus entry, immunogenicity, and pathogenicity (Li et al. 2016). Consequently, the S gene is considered an essential target for understanding the genetic relationships and epidemiological profiles of field PEDV isolates (Chen et al. 2013).

Handling editor: Min Cui (Executive Editor in Chief).

*Correspondence:

Liurong Fang
fanglr@mail.hzau.edu.cn

¹ National Key Laboratory of Agricultural Microbiology, College of Veterinary Medicine, Huazhong Agricultural University, Wuhan, China

² Key Laboratory of Preventive Veterinary Medicine in Hubei Province, The Cooperative Innovation Center for Sustainable Pig Production, Wuhan, China



© The Author(s) 2025. **Open Access** This article is licensed under a Creative Commons Attribution 4.0 International License, which permits use, sharing, adaptation, distribution and reproduction in any medium or format, as long as you give appropriate credit to the original author(s) and the source, provide a link to the Creative Commons licence, and indicate if changes were made. The images or other third party material in this article are included in the article's Creative Commons licence, unless indicated otherwise in a credit line to the material. If material is not included in the article's Creative Commons licence and your intended use is not permitted by statutory regulation or exceeds the permitted use, you will need to obtain permission directly from the copyright holder. To view a copy of this licence, visit <http://creativecommons.org/licenses/by/4.0/>. The Creative Commons Public Domain Dedication waiver (<http://creativecommons.org/publicdomain/zero/1.0/>) applies to the data made available in this article, unless otherwise stated in a credit line to the data.

PEDV can be classified into at least three major genotypes based on the sequence of the S gene: G1 (classical), G2 (variant), and S-INDEL (with insertions and deletions in the S gene). The prototype strain of G1 PEDV, CV777, was first identified in Europe in the 1970s (Wood 1977), with reports of its occurrence in China as early as the 1980s (Chen et al. 2010). However, the G1 PEDV only sporadically circulated in the swine population. The G2 (G2a, G2b and G2c) PEDV is a highly virulent variant that emerged in late 2010. Currently, G2 PEDV has become the dominant strain worldwide and circulates in swine farms across Asia and North America, resulting in enormous economic losses to the swine industry (Chen et al. 2011; Lin et al. 2016; Ojkic et al. 2015; Sun et al. 2015; Zhao et al. 2020).

The S-INDEL strain, represented by OH851, was initially identified in the United States in 2014 (Wang et al. 2014). Owing to its unique genetic characteristics, particularly the insertions and deletions in the S gene of S-INDEL strains compared with the prevalent G2 strain in the United States, this genotype was designated S-INDEL. Currently, S-INDEL PEDV is epidemic mainly in Europe and the United States (Boniotto et al. 2016; Chen et al. 2016a, b; Grasland et al. 2015; Mesquita et al. 2015; Stadler et al. 2015; Wang et al. 2014) and has also been reported in several Asian countries, such as South Korea and Japan (Kim et al. 2024; Lee and Lee 2014; Van Diep et al. 2015). In China, there were few reports of PEDV S-INDEL strain until 2021. Our group detected one S-INDEL-positive clinical sample in 2015 and determined its genome sequence (GenBank accession number KU847996). Intriguingly, the S-INDEL strain appeared to have been epidemic in China since 2021, with a total of 13 PEDV S-INDEL genome sequences from Chinese swine populations uploaded to NCBI since that time. However, there have been no reports of successful isolation of the S-INDEL strain in China until now.

In this study, we successfully isolated a PEDV S-INDEL strain, named EJS6, from a pig farm experiencing PED outbreaks in Jiangsu Province, China, in late 2022. We also determined the genome sequence of EJS6 and its genetic characterization. Additionally, we investigated the pathogenicity of the EJS6 strain in 5-day-old suckling piglets to enhance our understanding of the pathogenesis of the PEDV S-INDEL strain in China.

Results

Isolation and identification of the PEDV S-INDEL strain EJS6

In 2022, a widespread outbreak of piglet diarrhea and mortality occurred on a pig breeding farm in Jiangsu Province, China. Intestinal samples were collected from piglets with severe diarrhea and tested for known viruses

associated with piglet diarrhea, including PEDV, transmissible gastroenteritis virus (TGEV), porcine deltacoronavirus (PDCoV), and porcine rotavirus (PoRV), via RT-PCR with specific primers. The results revealed that all the tested intestinal samples were positive for PEDV (Fig. 1A), indicating that the piglet diarrhea observed at this farm might have been caused by PEDV. To further identify the genotype of PEDV responsible for this outbreak, we sequenced the S gene from the collected intestinal samples. The analysis revealed that the S gene exhibited unique insertions and deletions similar to those of the S-INDEL strains reported in Europe and the United States.

Given that there have been no prior reports of successful isolation of the PEDV S-INDEL strain in China, we attempted to isolate the virus from the collected intestinal samples. After three blind passages, typical cytopathic effects (CPEs), including cell fusion and syncytium formation, were observed. An indirect immunofluorescence assay (IFA) demonstrated that the PEDV N-specific monoclonal antibody (mAb) produced a specific fluorescence reaction in Vero cells inoculated with the isolated virus, whereas no fluorescence signal was detected in mock-infected cells (Fig. 1B), confirming the successful isolation of PEDV. The S gene was cloned from the isolated PEDV, and its sequence was determined. Sequencing analysis further confirmed that the isolated PEDV belongs to the S-INDEL genotype and was designated EJS6.

Phylogenetic analysis of the whole-genome and S gene sequences of EJS6

To better understand the genetic evolution of the isolated EJS6 strain, we determined its whole-genome sequence (GenBank accession number PQ768103). Phylogenetic trees based on the whole-genome and S gene sequences classified the EJS6 strain into the PEDV S-INDEL genotype, which presented 98.6% similarity to the whole genome of the reference S-INDEL strain OH851 (Fig. 2A) and 97.6% nucleotide similarity for the S gene (Fig. 2B). Additionally, we examined the reported timeline of PEDV S-INDEL strains and noted a significant increase in their prevalence, particularly among strains situated on the same evolutionary branch as EJS6. This observation prompted us to explore the molecular genetic characteristics of the PEDV S-INDEL genotype. By utilizing the PEDV S gene sequences, we constructed a Bayesian phylogenetic tree, which revealed the existence of three distinct groups among the S-INDEL strains. Notably, our analysis traced the classic S-INDEL strains back to 2010, whereas another group, predominantly consisting of strains from Europe, originated approximately 2008.

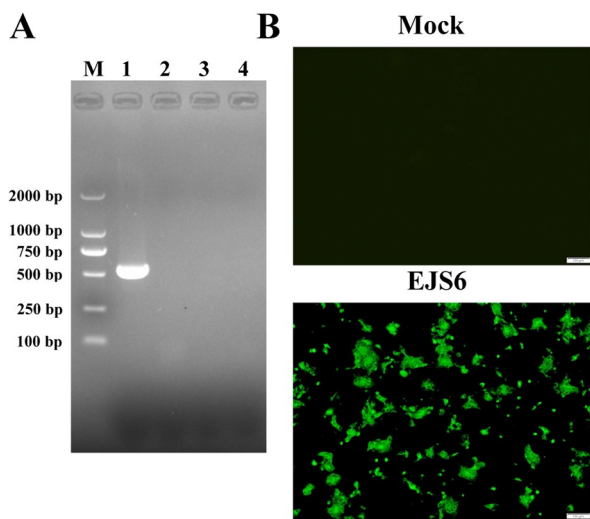


Fig. 1 Virus isolation and identification of the PEDV S-INDEL strain EJS6. **A** RT-PCR was conducted to detect the presence of PEDV, PDCoV, TGEV, and PoRV in the collected intestinal samples. M: 2,000 bp DNA marker; lane 1: PEDV; lane 2: PDCoV; lane 3: TGEV; lane 4: PoRV. **B** Identification of EJS6 in Vero cells *via* indirect immunofluorescence assay using a PEDV N-specific mAb. The fluorescence images were captured via a fluorescence microscope (Olympus). Scale bars, 100 μ m

In contrast, more recent outbreaks of S-INDEL strains, mainly from China, formed a distinct and independent group, highlighting significant genetic divergence within the PEDV S-INDEL genotype (Fig. 2C). Furthermore, Bayesian skyline plot (BSP) analysis indicated that the effective population size and relative genetic diversity of the PEDV S-INDEL lineage increased steadily until approximately 2013. This growth plateaued during the period from 2015–2020, followed by a decline in both population size and genetic diversity (Fig. 2D). These findings suggest that the PEDV S-INDEL genotype may be poised for localized outbreaks in the near future.

Codon usage patterns in PEDV S-INDEL strains

The results from the abovementioned phylogenetic tree analysis classified the PEDV S-INDEL strains into three distinct groups, highlighting significant diversity within the PEDV S-INDEL genotype. To further elucidate the factors contributing to the formation of the three S-INDEL groups, we analyzed the codon usage patterns of the S gene of the PEDV S-INDEL strains. The results revealed distinct clustering patterns among the three groups: group 1 (classic European and American strains), group 2 (newly emerged European strains), and group 3 (main strains from China) (Fig. 3A). Furthermore, the effective number of codons (ENC) analysis indicated that

the average ENC value of the S gene of S-INDEL strains was 47, exceeding the generally accepted threshold of 35 (Lu et al. 2023), which serves as a cutoff for determining whether a gene is influenced by mutation pressure or other factors, such as translational selection (Fig. 3B). As illustrated in Fig. 3C, all data points representing the ENC values of the S gene of the S-INDEL strains fell below the expected curve, suggesting that mutation pressure is not the sole factor influencing the codon usage bias (CUB) of the S gene. Moreover, group 3 did not overlap with groups 1 and 2, indicating a significant impact of natural mutation on group 3. Therefore, the CUB of the S gene of S-INDEL strains is shaped by both mutation pressure and natural selection.

In addition, parity rule 2 (PR2) analysis revealed that $A \neq U$ and $C \neq G$ in the S gene of the S-INDEL strains, suggesting that the influences of mutation pressure and natural selection are not equal in shaping the codon usage of the S gene (Fig. 3D). Furthermore, we calculated the relationships between the GC3s and GC12s of three groups of S-INDEL strains in the S gene. The correlation coefficients of the group 1, group 2, and group 3 strains were 0.057, 0.168 and 0.091, respectively. Consequently, the natural selection restriction rates of the S gene in these three groups were 94.3%, 83.2%, and 90.9%, respectively (Fig. 3E). These results suggest that natural selection is the primary factor shaping the CUB of the S gene. To further investigate the impact of selection pressure on the S protein of the S-INDEL strains, we identified four amino acid residues (aa 83, 113, 114 and 156) in a positively selected state (Table 1). These selected amino acids are located in the D0 region of the PEDV S1 protein. Previous studies have reported that the D0 region of the PEDV S1 protein is associated with the sugar-binding ability of the virus (Deng et al. 2016). Therefore, our findings imply that the ability of PEDV to utilize carbohydrates for host entry may be linked to these four sites.

Characteristic amino acid changes in the S protein of the PEDV S-INDEL strains

Mutations in the S protein of coronaviruses can significantly influence their receptor-binding efficiency and immunogenicity (Li et al. 2023; Rattanapitit et al. 2021). The S gene across different PEDV strains consistently presented insertions and deletions, which were particularly pronounced in the PEDV S-INDEL strains. By comparing the amino acid sequence of the S protein of the newly isolated EJS6 strain with those of other PEDV reference strains, including those from groups G1a/b, G2a/b/c and other PEDV S-INDEL strains (Fig. 4), we identified three distinct regions characterized by insertions and deletions in the amino acid sequence of the S protein. These regions are located at amino acid positions

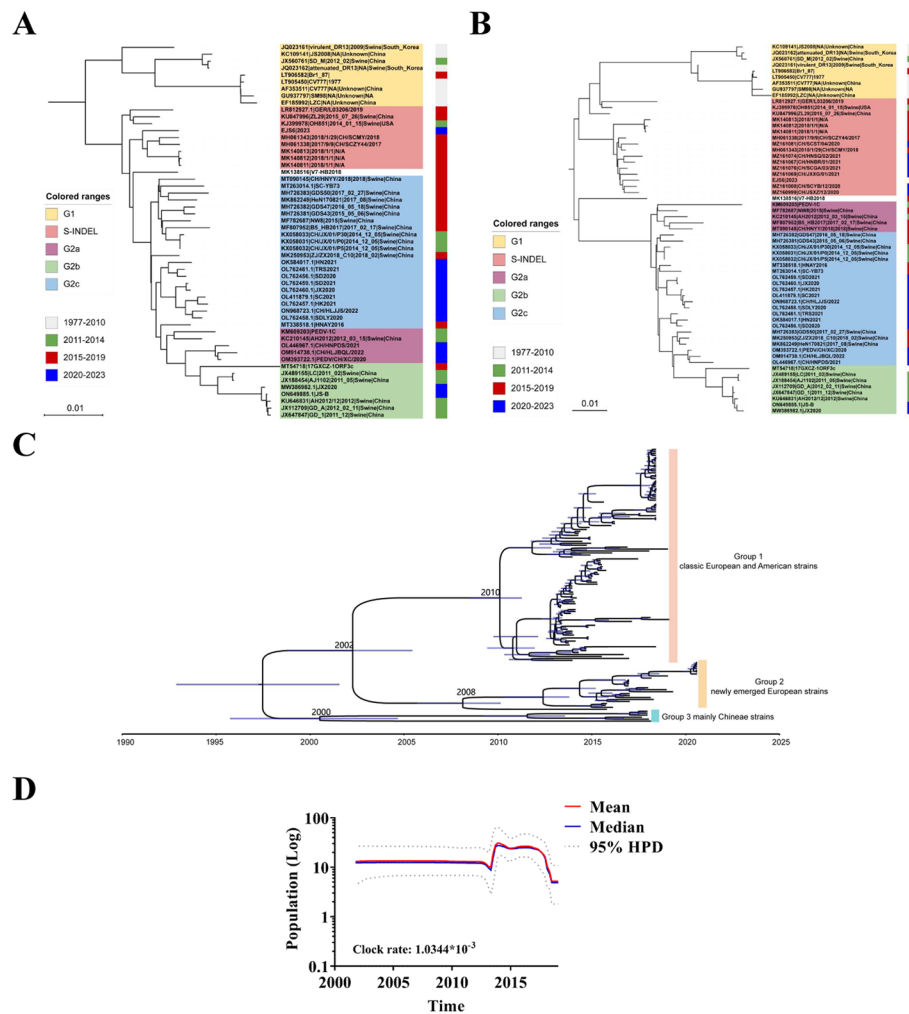


Fig. 2 Phylogenetic tree and Bayesian spatiotemporal speculation of the PEDV S-INDEL strains. **A** and **B** Phylogenetic trees were constructed via the maximum likelihood (ML) approach on the basis of the complete genome sequences (**A**) and S gene sequences (**B**) of PEDV. Different colors denote the defined clusters: yellow, PEDV G1; red, PEDV S-INDEL; purple, PEDV G2a; green, PEDV G2b; blue, PEDV G2c. The colored blocks on the right illustrate the temporal distribution of strains across various timeframes. **C** An MCC tree of the S gene was constructed via BEAST V. 1.8.2. The x-axis represents the time in years. The colored blocks on the right correspond to different groups within the PEDV S-INDEL strains. **D** Demographic history inferred via a skyline coalescent tree prior. The interval formed by the dashed line represents the 95% HPD of the product of generation time and effective population size $N_e(t)$. The red line indicates the mean, and the blue line represents the median

54–65, 136–143, and 156–169. At positions 54–65, both the S-INDEL and G1 strains exhibited identical patterns of deletions and mutations, establishing this as a critical protein sequence marker for differentiating S-INDEL strains from G2a/b/c strains. In contrast, the Chinese S-INDEL strains represented by EJS6 presented unique protein sequence markers in the regions spanning amino acids 136–143 and 156–169, distinguishing them from other S-INDEL strains. Notably, Chinese S-INDEL strains exhibited a distinct pattern of deletions and mutations in the region of amino acids 136–143, indicating a greater degree of variability in this region.

Comparison of the infection properties of EJS6 and EHuB4 in Vero cells

To further understand the infection properties of EJS6 in Vero cells, we used a representative PEDV G2c strain, EHuB4, which was isolated in China in 2020 as a control. Both EJS6 and EHuB4 were analyzed at the 10th passage. Compared with those in the EHuB4 strains, the syncytia formed in the EJS6-infected Vero cells were smaller (Fig. 5A), a finding that was further corroborated by IFA with a PEDV S-specific mAb (Fig. 5B). Plaque assays demonstrated significantly smaller plaque sizes for EJS6 compared to EHuB4 (Fig. 5C, D). Additionally, we

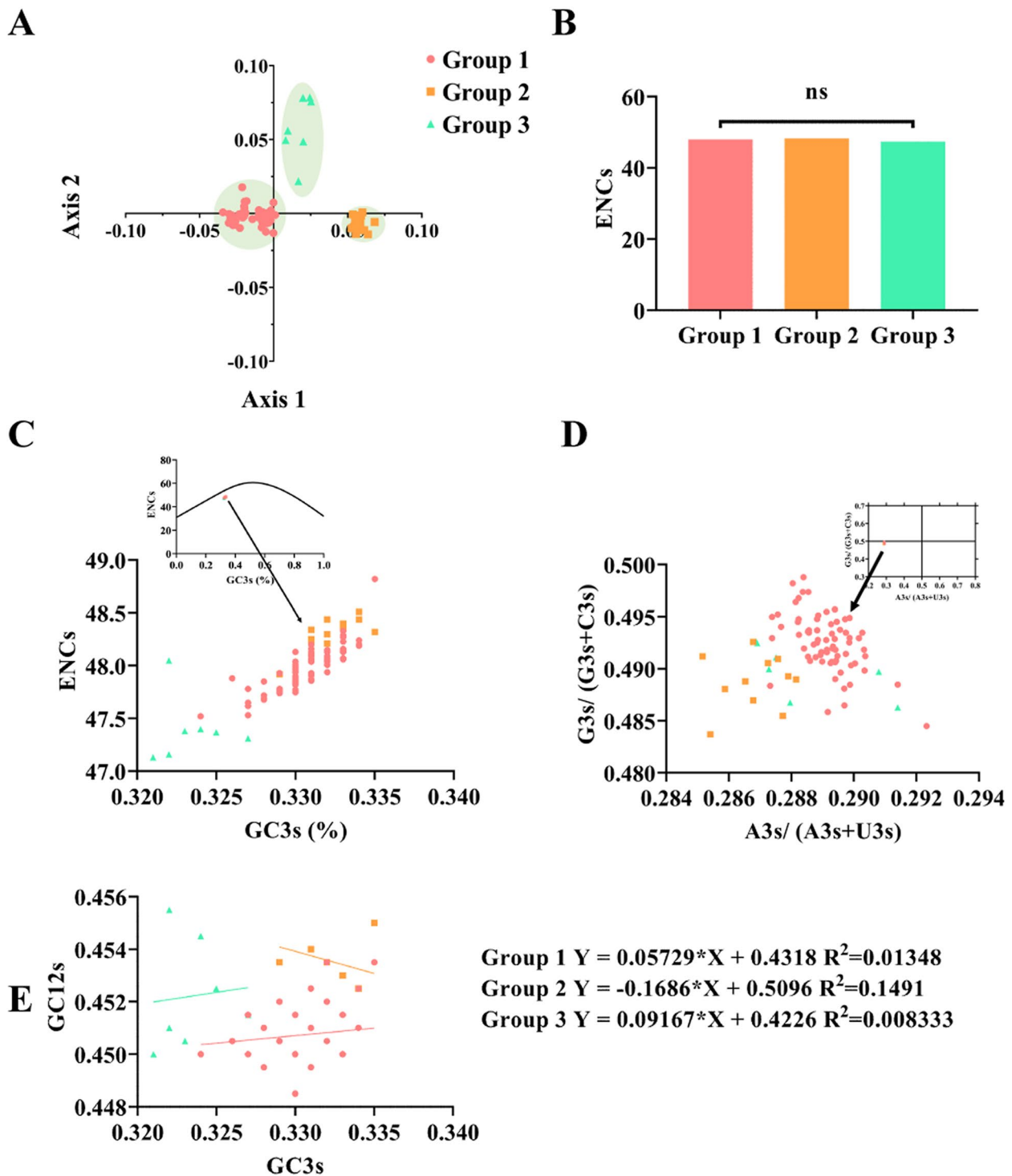


Fig. 3 Codon usage pattern analysis of the S gene of the PEDV S-INDEL strains. **A** Principal component analysis (PCA) of the PEDV S-INDEL S gene. **B** and **C** Effective number of codons (ENC) (**B**) and ENC-GC3s plot (**C**) of the PEDV S-INDEL S gene. The curve indicates the standard expected values. The differently colored circles represent the observed ENC-GC3 values for individual clusters. **D** Diagonal analysis of the S gene of the PEDV S-INDEL strains. **E** Neutral analysis of the S gene of different S-INDEL strains, with each point representing an independent PEDV S-INDEL strain. Groups 1, 2 and 3 are indicated in red, yellow and green, respectively

compared the proliferation dynamics of these two PEDV strains under identical infection conditions. The results revealed that EJS6 reached its peak titer at 18 h post infection (hpi), with a viral titer of $10^{4.25}$ TCID₅₀/mL, whereas EHuB4 peaked at 24 hpi, with a viral titer of up to $10^{8.0}$ TCID₅₀/mL (Fig. 5E). These findings indicate that EJS6 has a lower replication capacity in vitro than EHuB4 does.

Comparison of the pathogenicity of EJS6 and EHuB4 in neonatal piglets

To compare the pathogenicity of EJS6 and EHuB4 in piglets, 5-day-old piglets were orally inoculated with $5 \times 10^{4.2}$ TCID₅₀ of either EJS6 or EHuB4, and the piglets inoculated with DMEM served as the control group (Fig. 6A). Piglets in the PEDV-inoculated groups began to develop severe diarrhea at 2 days post inoculation (dpi) and died at 4 dpi (Table 2). Notably, despite mortality events occurring in both PEDV-inoculated groups, there were notable differences in the morbidity and mortality timelines. In the EHuB4 group, mortality was observed on days 7, 8 and 9 post infection, with two out of five piglets dying on day 7 and one out of five on day 8, and all five piglets died within 9 days of infection. Conversely, the EJS6 group experienced earlier mortality, with one piglet (1/5) died on day 4 post infection, followed by another piglet (2/5) that died on day 7. Importantly, the remaining three piglets in the EJS6 group survived until the end of the experiment (Fig. 6B). Similarly, the RT-qPCR results revealed that the peak number of viral RNA copies in the anal swabs of the EHuB4 group was $10^{11.82}$ copies/mL, whereas it was $10^{11.89}$ copies/mL in the EJS6 group (Fig. 6C). Furthermore, the EJS6 group presented milder intestinal lesions than did the EHuB4 group, which presented typical gross intestinal lesions (Fig. 6D).

Histopathological analysis of the duodenum, jejunum, and ileum in the control group revealed a well-preserved tissue structure characterized by intact villus architecture and the absence of obvious abnormalities. In contrast, the intestinal epithelium of the duodenum, jejunum, and ileum in the EHuB4 group exhibited significant atrophy, characterized by shortened, blunted, and fused villi. In the EJS6 group, notable villus shortening was observed exclusively in the jejunum and ileum (Fig. 7A). The immunohistochemistry results revealed a substantial presence of PEDV antigen-positive signals in the small intestinal villous epithelial cells of the jejunum and ileum in the EHuB4 group, whereas in the EJS6 group, positive signals were detectable only in the ileum. These findings suggest that the pathogenicity of the EJS6 strain is weaker than that of the EHuB4 strain, indicating distinct tissue tropism between the two strains (Fig. 7B).

Discussion

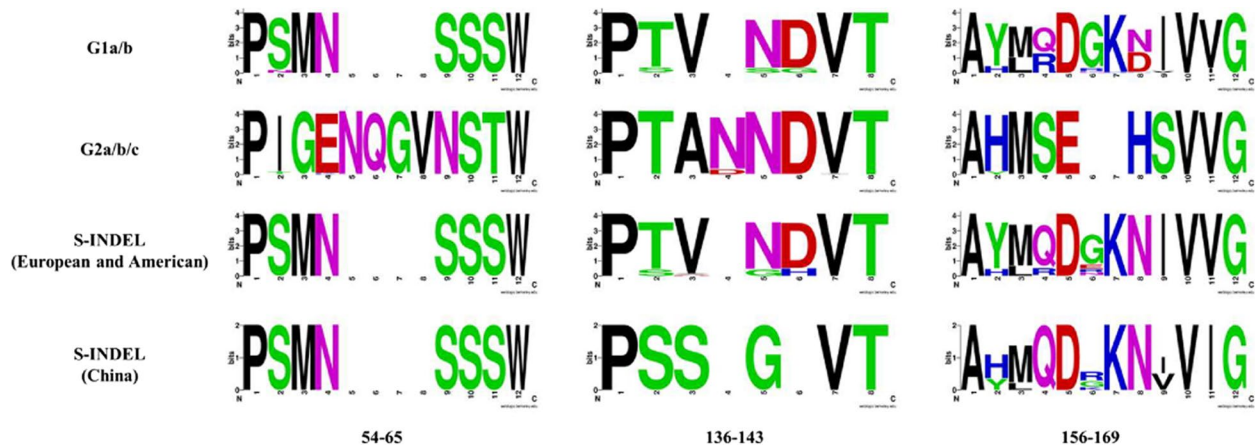
Originally reported in Europe, PEDV has become the most important intestinal pathogen affecting swine in China, particularly since the emergence of G2 PEDV variants in 2010 (Chen et al. 2012; Lin et al. 2016). In 2013, the outbreak of PEDV S-INDEL variants in the United States and neighboring countries, including Canada and Mexico, led to substantial economic losses (Ojkic et al. 2015; Vlasova et al. 2014). The dynamic evolution of PEDV poses formidable challenges for the prevention and control of this disease. Therefore, obtaining timely insights into clinical epidemic strains, as well as variation patterns and identifying vaccine candidates are crucial for the effective prevention and control of PED.

In this study, we successfully isolated a PEDV S-INDEL strain, designated EJS6. To our knowledge, this is the first report of the isolation of a PEDV S-INDEL strain in China. The results of in vitro replication kinetics demonstrated that the proliferation capability of the EJS6 strain was lower than that of the EHuB4 strain, with a viral titer $10^{3.75}$ TCID₅₀/mL lower than that of the EHuB4 strain. The lower viral titer appears to be a common characteristic of all S-INDEL isolates because the reported titers of the two S-INDEL strains in previous studies ranged from $10^{4.5}$ to $10^{5.0}$ TCID₅₀/mL (Gallien et al. 2019; Schumacher et al. 2022). However, the limited number of isolated S-INDEL strains currently hinders our ability to definitively establish whether a lower viral titer is a universal property among all S-INDEL isolates. Additionally, the syncytia and plaques formed by the EJS6 strain were smaller than those formed by the EHuB4 strain. Previous studies have reported that the S protein of coronaviruses is associated with viral replication capability, cell fusion, and syncytial formation (Sato et al. 2011; Wanitchang et al. 2019). Thus, we systematically analyzed the molecular differences in the S protein and found that the amino acid region spanning positions 54–65 in the S protein can serve as a key molecular marker distinguishing S-INDEL strains from G2a/b/c strains. Notably, the Chinese S-INDEL strains represented by EJS6 exhibit a unique pattern of deletions and mutations in the amino acid region 136–143, indicating greater variability in this region. However, whether these deletions and mutations contribute to the observed variations in in vitro replication characteristics remains to be determined through the viral reverse genetics system.

A previous study revealed that PEDV S-INDEL strains may have originated from recombination events prior to 2010, with a backbone similar to that of G2 strains and the 5' terminus of the S gene sequence derived from G1 strains, and the S genes of these

Table 1 Positive selection sites in the S protein of PEDV S-INDEL strains

Protein	aa	FEL		SLAC		FUBAR		MEME	
		dN-ds	p-Value	dN-ds	p-Value	dN-ds	Post. Pro	ω	p-Value
Spike	83	12.183	0.0181	26.37367	0.019411	32.184	0.991	>100	0.01
	113	7.778	0.0263	18.87243	0.039702	20.692	0.987	>100	0
	114	9.518	0.0201	18.17151	0.055814	29.791	0.996	>100	0.03
	156	25.795	0.0114	39.57619	0.007348	32.898	0.955	>100	0

**Fig. 4** Characteristic amino acids in the S protein of different PEDV genotypes. Alignments of amino acid sequences at positions 54–65, 136–143 and 156–169 of the S proteins from PEDV genotypes G1a/b and G2a/b/c, as well as American and European S-INDEL strains and Chinese S-INDEL strains

recombinants might have evolved independently, leading to genetic drift under field conditions (Guo et al. 2019). However, the clinical symptoms caused by different PEDV S-INDEL strains appear to be inconsistent. Pathogenicity experiments conducted in both clinical and laboratory settings in the United States have demonstrated that the S-INDEL strain results in milder clinical symptoms (Chen et al. 2016a, b; Wang et al. 2014). Conversely, a PEDV S-INDEL outbreak in Germany (99.4% homology to the US S-INDEL strain OH851) reported diverse clinical manifestations, including unexpectedly high mortality rates in suckling piglets on one of the farms (Mesquita et al. 2015; Stadler et al. 2015). These discrepancies may reflect inherent pathogenicity variations among S-INDEL strains. Notably, the pathogenicity of the EJS6 strain appears to fall between the reported values from Europe and the United States. Although the pathogenicity of the S-INDEL strain EJS6 was somewhat lower than that of the EHuB4 strain, it still resulted in a 100% incidence rate and a 40% fatality rate in laboratory settings. Compared with the EHuB4 strain, which exhibited PEDV antigen distribution in both

the jejunum and ileum, the EJS6 strain demonstrated antigen localization restricted to the ileum. Previous studies have indicated that the mechanisms underlying the pathogenicity and tissue tropism of PEDV may be related to the N-terminal sequence of the S protein (Hou et al. 2017; Suzuki et al. 2016, 2018); however, further evidence is needed to support this conclusion. Other studies have reported that pregnant sows infected with the S-INDEL strain can confer a certain degree of protection to newborn piglets infected with the PEDV G2a U.S. strain (Goede et al. 2015). An animal experiment with weaned piglets demonstrated that both the American PEDV prototype strain and the PEDV S-INDEL strain could provide homologous or heterologous protection to each other (Chen et al. 2016a, b; Lin et al. 2015a, b). Additionally, 3–4-day-old piglets infected with the S-INDEL strain exhibited resistance to infection from the American prototype strain (Lin et al. 2015a, b). Therefore, the EJS6 strain isolated in this study has the potential to be developed into a promising vaccine candidate capable of providing cross-protection against G2 PEDV infections.

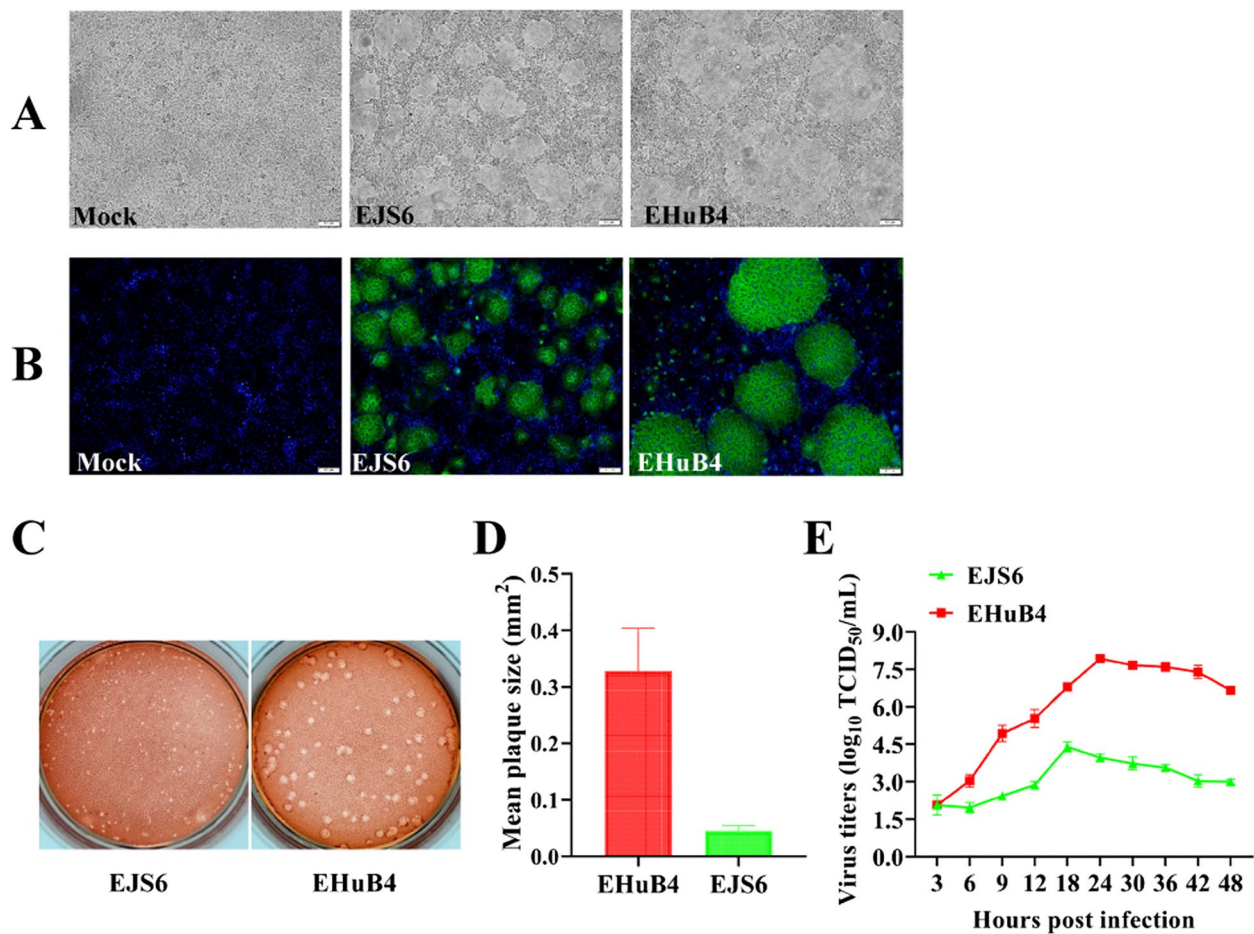


Fig. 5 Comparison of the infection properties of EJS6 and EHUB4. **A** Cytopathic effects (CPEs) in Vero cells infected with PEDV EJS6 or EHUB4 (MOI=0.1) at 12 hpi. Scale bars, 100 μ m. **B** Formation of syncytia in Vero cells infected with EJS6 and EHUB4. An indirect immunofluorescence assay was conducted with a PEDV S-specific mAb. Scale bars, 100 μ m. **C** Plaques of EJS6 and EHUB4 in Vero cells by plaque assay. **D** The mean plaque sizes of EJS6 and EHUB4 were determined by measuring the bounding rectangle areas of seven randomly selected plaques. **E** Growth kinetics of EJS6 and EHUB4 in Vero cells

Conclusion

In this study, we successfully isolated the first Chinese PEDV S-INDEL strain, EJS6, from clinical intestinal samples and characterized its genetic variation. We also compared the infection properties and pathogenicity of EJS6 with those of the EHUB4 strain, revealing that the PEDV S-INDEL strain EJS6 has a lower replication capability, results in the formation of smaller syncytia in Vero cells, and has lower pathogenicity in neonatal piglets. This study provides critical insights into the genetic diversity and attenuated pathogenicity of emerging S-INDEL strains, advancing our understanding of PEDV epidemiology in China.

Methods

Sample collection, treatment and detection

Small intestine samples from piglets with severe diarrhea were collected from a farm in Jiangsu Province, China, in 2022. These samples were diluted threefold with phosphate-buffered saline (PBS), homogenized, and then centrifuged at 12,000 rpm for 10 min at 4°C. The resulting supernatants were filtered through a 0.22- μ m pore size filter (Millipore, USA) and preserved at -80°C for subsequent virus detection and isolation. For the detection of PEDV, total RNA was extracted and reverse transcribed into cDNA *via* the

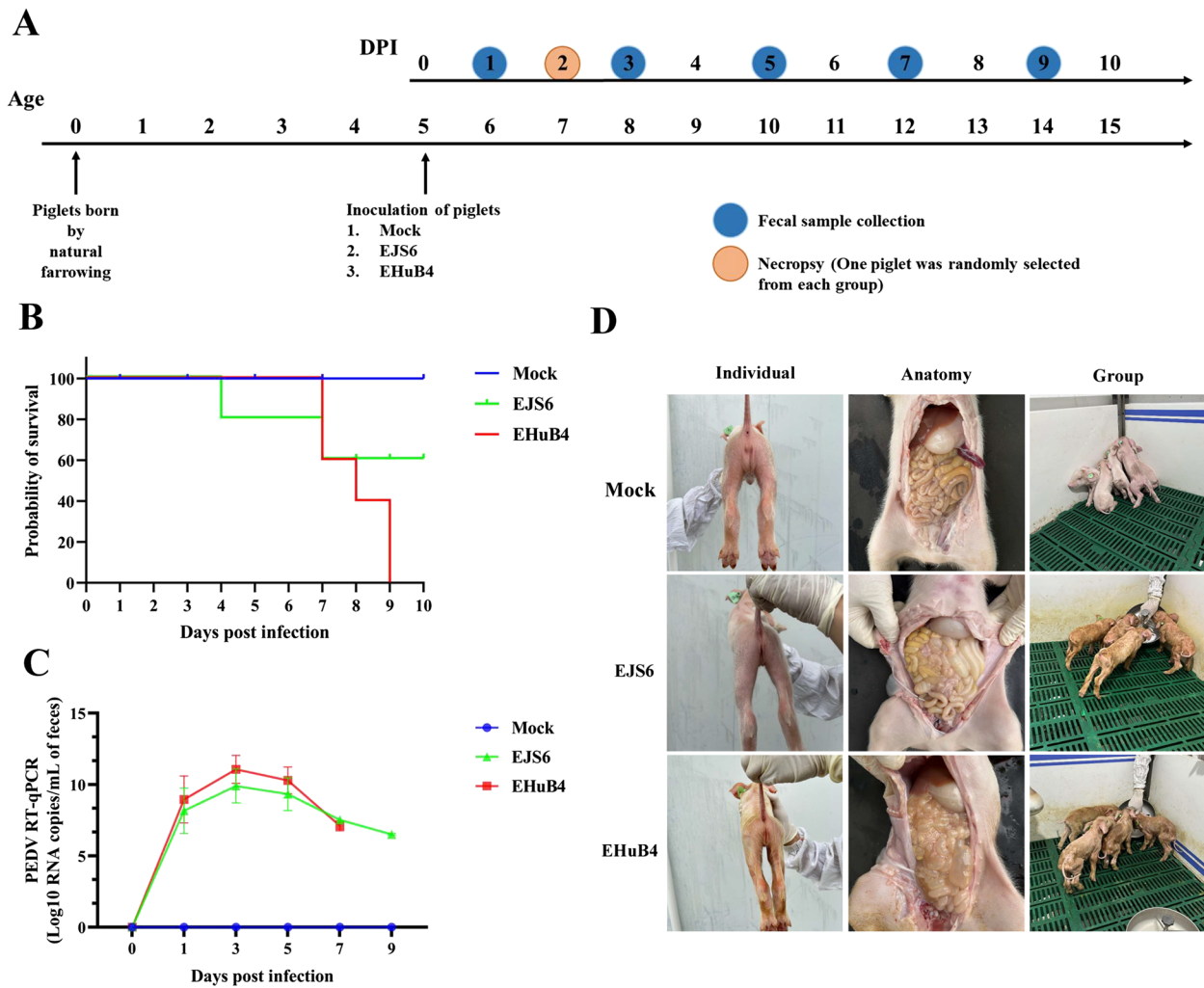


Fig. 6 Pathogenicity of EJS6 and EHuB4 in 5-day-old piglets. **A** Schematic diagram of the animal experiment. Five-day-old piglets (six piglets per group) were inoculated orally with either EJS6 or EHuB4 ($5 \times 10^{4.2}$ TCID₅₀/piglet). Piglets that received DMEM orally served as the control group. Two days postinfection, one piglet from each group was randomly selected for euthanasia to examine intestinal lesions. The remaining piglets were monitored for survival rates and fecal virus shedding over a period of 10 days. **B** The percentage of surviving piglets in each group. **C** Fecal virus shedding was measured in piglets at 0, 1, 3, 5, 7 and 9 days post infection. **D** Clinical symptoms and gross anatomical lesions observed in piglets after infection. Piglet photos of individuals and anatomy were captured 48 h post infection, whereas photos of the groups were taken on the fourth day following piglet infection

TRIzol method and a Vazyme RNA reverse transcription kit following the manufacturer’s instructions. PCR was subsequently conducted with primers targeting the S gene of PEDV. The sequences of the primers are listed in Table S1.

Cell culture and virus isolation

Vero cells (ATCC CCL-81) were cultured in Dulbeco’s modified Eagle’s medium (DMEM; Gibco, USA)

supplemented with 10% fetal bovine serum (FBS). Confluent Vero cells in a six-well cell culture plate were washed three times with PBS and then inoculated with 200 μL of the treated small intestine sample. After adsorption for 2 h, the inoculum was removed, and the cells were maintained in fresh DMEM containing 10 μg/mL trypsin. The cells were observed daily. If a typical CPE was observed, the cell cultures were collected and stored at -80°C. Otherwise, the cell cultures were collected, and blind passage was performed for three passages until a typical CPE appeared.

Table 2 Clinical observation records of 5-day-old piglets infected with PEDV strain EJS6 or EHUB4

dpi	Clinical observation	EJS6			Clinical observation	EHUB4		
		Fecal consistency				Fecal consistency		
		Normal	Mild diarrhea	Watery diarrhea		Normal	Mild diarrhea	Watery diarrhea
1	All active and eating well	5/5	0/5	0/5	All active, 60% with vomiting and anorexia	2/5	3/5	0/5
2	All active, 40% with vomiting and anorexia	2/5	1/5	2/5	All active, 100% with vomiting	0/5	5/5	0/5
3	All with lethargy, vomiting and anorexia	0/5	0/5	5/5	All with lethargy, vomiting and anorexia	0/5	0/5	5/5
4		0/5	0/5	5/5		0/5	0/5	5/5
5	All with lethargy and anorexia	0/4	0/4	4/4	All with lethargy and anorexia	0/5	0/5	5/5
6		0/4	3/4	1/4		0/5	0/5	5/5
7		0/3	3/3	0/3		0/3	1/3	2/3
8	All with lethargy, 66% with anorexia	0/3	3/3	0/3	All died	0/2	1/2	1/2
9		0/3	3/3	0/3		0	0	0
10		1/3	2/3	0/3				

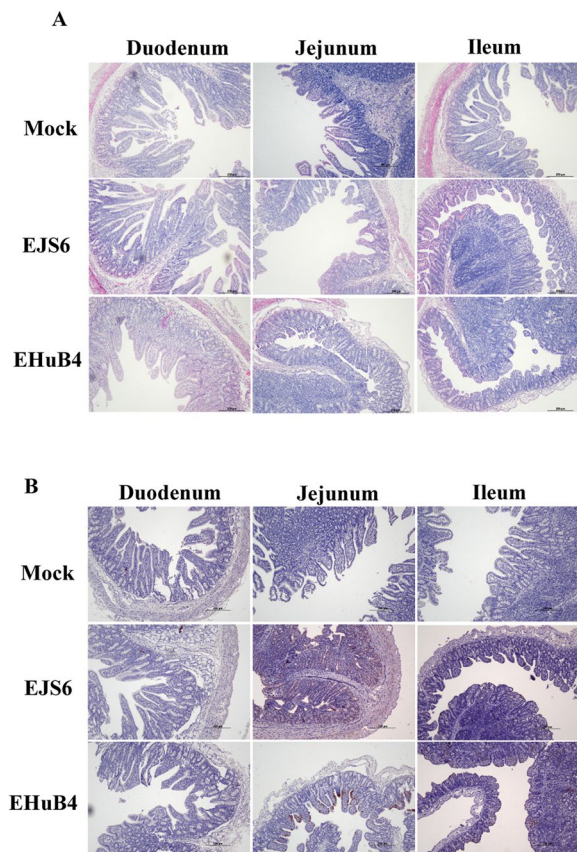


Fig. 7 Histopathological examination of piglets after PEDV infection. Hematoxylin and eosin (H&E) staining (**A**) and immunohistochemical analysis (**B**) of the duodenum, jejunum, and ileum collected from piglets necropsied at 2 days post infection. All the tissue sections were observed under 100× magnification. Scale bars, 200 μm

Indirect immunofluorescence assay (IFA)

Cells infected or mock-infected with PEDV were washed with PBS, fixed with 4% paraformaldehyde and permeabilized with cold methanol. After being blocked with 5% bovine serum albumin, the cells were incubated with a mAb against the PEDV N or S protein and then with a fluorescein isothiocyanate (FITC)-conjugated goat anti-mouse IgG antibody. Finally, the nuclei were stained with 0.01% 4',6-diamidino-2-phenylindole (DAPI), and the fluorescence images were visualized via a fluorescence microscope (Olympus).

Viral multistep growth curve

Vero cells in 12-well plates were inoculated with PEDV at an MOI of 0.001. The virus suspensions were collected at 3, 6, 9, 12, 18, 24, 30, 36, 42 and 48 hpi. The 50% tissue culture infectious dose of these collected samples was subsequently assayed as described previously (Nemeth et al. 2018).

Sequence and phylogenetic analysis

The complete genome sequence of the isolated EJS6 strain was determined via the paired primers listed in Table S1. A total of 53 complete genome sequences and 60 S gene sequences of PEDV were retrieved from the NCBI GenBank database (<https://www.ncbi.nlm.nih.gov/>) to serve as reference sequences. Phylogenetic trees were constructed for both the whole-genome sequences and the S gene sequences. Detailed information about these sequences is provided in Table S2. Sequence alignment was conducted via MAFFT V.7.402 (Katoh and Standley 2013) to compare nucleotide and amino acid

sequences. Maximum likelihood (ML) phylogenetic trees were generated via IQ-TREE V.1.6.5 (Nguyen et al. 2015). The spatiotemporal dynamics of PEDV were inferred within a Bayesian framework via BEAST V. 1.8.2 (Baele et al. 2017). Additionally, a coalescent Bayesian skyline model for the tree topologies was employed to estimate the effective population size over time. One chain with a length of 1×10^9 converged to indistinguishable posterior distributions. We assessed convergence and mixing *via* Tracer software (V. 1.7) (Rambaut et al. 2018), which implemented a burn-in period of 10% of the total chain length. All the parameter estimates yielded an effective sampling size >200 . The resulting phylogenetic trees were visualized with iTOL V. 4 (Interactive Tree of Life, <http://itol.embl.de/>).

Codon usage patterns and positive selection analysis

The ENC, neutrality plot, and parity rule 2 bias plot for the encoded sequence of each PEDV S-INDEL strain were calculated *via* the Galaxy website (<https://galaxy.Pasteur.fr>) and CodonW software. An ML tree was reconstructed on the basis of nonrecombinant sequences via Datamonkey (<http://www.datamonkey.org/>). The methods employed to scrutinize positive amino acid sites included single likelihood ancestor counting (SLAC), fixed effects likelihood (FEL), mixed effects model of evolution (MEME) and fast unconstrained Bayesian approximation (FUBAR) (Kosakovsky Pond and Frost 2005; Murrell et al. 2012, 2013; Smith et al. 2015). Codons were deemed under selection if highlighted by at least three methods. Sites identified by a minimum of two algorithms were considered conservatively indicative of positive selection.

Animal experiments

Eighteen 5-day-old piglets sourced from a PEDV-negative farm were randomly assigned to three groups, with six piglets per group. The first group was orally administered the EJS6 strain ($5 \times 10^{4.2}$ TCID₅₀ per piglet), the second group was orally administered the EHuB4 strain at the same dose as a positive control, and the negative control group was orally administered the same volume (5 mL) of DMEM. After inoculation, the mental state and fecal condition of the piglets were observed and assessed daily for 10 days (Fig. 6A). Anal swabs were collected each day, and virus shedding was detected via real-time reverse transcriptase quantitative PCR as described previously (Ding et al. 2023). On the second day post virus challenge, one piglet from each group was randomly selected for euthanasia to examine intestinal lesions, while the remaining piglets were euthanized on the tenth day post challenge.

Gross and histopathological examination

Tissue samples from the duodenum, jejunum and ileum were collected from euthanized piglets and then dehydrated, embedded and sectioned. The sections were used for histological and immunohistochemical examinations as described previously (Dong et al. 2016).

Statistical analysis

Statistical analysis was conducted *via* Student's t test *via* GraphPad Prism 10.1.0 (GraphPad Software, CA, USA). $P < 0.05$ was considered statistically significant.

Abbreviations

BSP	Bayesian skyline plot
CPEs	Cytopathic effects
CUB	Codon usage bias
DAPI	4',6-Diamidino-2-phenylindole
dN	Nonsynonymous substitutions
dpi	Days postinoculation
dS	Synonymous substitutions
FEL	Fixed effects likelihood
ENC	Effective number of codons
FBS	Fetal bovine serum
FITC	Fluorescein isothiocyanate
FUBAR	Fast unconstrained Bayesian approximation
H&E	Hematoxylin and eosin
hpi	Hour postinfection
IFA	Indirect immunofluorescence assay
mAb	Monoclonal antibody
MEME	Model of evolution
ML	Maximum likelihood
MOI	Multiplicity of infection
PBS	Phosphate-buffered saline
PCA	Principal component analysis
PDCoV	Porcine deltacoronavirus
PEDV	Porcine epidemic diarrhea virus
PR2	Parity Rule 2
PoRV	Porcine rotavirus
SLAC	Single likelihood ancestor counting
TGEV	Transmissible gastroenteritis virus

Supplementary Information

The online version contains supplementary material available at <https://doi.org/10.1186/s44149-025-00160-3>.

Supplementary Material 1: Table S1. Complete genomic and spike gene-specific primers for PEDV and RT-PCR detection primers for common porcine diarrhea viruses.

Supplementary Material 2: Table S2. Genomic and spike gene sequence analysis of porcine epidemic diarrhea virus (PEDV): A comprehensive dataset of 53 complete genomes and 60 spike gene sequences.

Acknowledgements

We would like to thank the National Key Laboratory of Agricultural Microbiology Core Facility for assistance with microscopy.

Authors' contributions

Yiye Zhang: Conceptualization, methodology, investigation, data curation, writing – original draft. Jiahui Guo: Methodology, Bioinformatics analysis, Writing – original draft. Qi Yang: Methodology, bioinformatics analysis. Tong Zhuang: Methodology, Investigation. Shaobo Xiao: Conceptualization, Resources, Supervision, Writing – review & editing. Liurong Fang: Conceptualization, project administration, resources, supervision, writing, review, and editing. All the authors read and approved the final manuscript.

Funding

This work is supported by the National Key Research and Development Program of China (2022YFD1800801).

Data availability

The datasets used or analyzed during the current study are available from the corresponding author upon reasonable request.

Declarations**Ethics approval and consent to participate**

In this study, all piglets were cared for in accordance with the guidelines set forth by the Regulations for the Administration of Affairs Concerning Experimental Animals established by the Ministry of Science and Technology of China. The experimental procedures were conducted following protocols approved by the Scientific Ethics Committee of Huazhong Agricultural University (Ethics Approval Number: HZAUSW-2023-0051).

Consent for publication

Not applicable.

Competing interests

The authors declare that there are no conflicts of interest associated with this manuscript.

Received: 12 December 2024 Accepted: 9 February 2025

Published online: 17 March 2025

References

- Baele, G., P. Lemey, A. Rambaut, and M.A. Suchard. 2017. Adaptive MCMC in Bayesian phylogenetics: An application to analyzing partitioned data in BEAST. *Bioinformatics* 33: 1798–1805. <https://doi.org/10.1093/bioinformatics/btx088>.
- Boniotti, M.B., A. Papetti, A. Lavazza, G. Alborali, E. Sozzi, C. Chiapponi, S. Faccini, P. Bonilauri, P. Cordioli, and D. Marthaler. 2016. Porcine epidemic diarrhea virus and discovery of a recombinant swine enteric coronavirus, Italy. *Emerging Infectious Diseases* 22: 83–87. <https://doi.org/10.3201/eid2201.150544>.
- Chen, J., C. Wang, H. Shi, H. Qiu, S. Liu, X. Chen, Z. Zhang, and L. Feng. 2010. Molecular epidemiology of porcine epidemic diarrhea virus in China. *Archives of Virology* 155: 1471–1476. <https://doi.org/10.1007/s00705-010-0720-2>.
- Chen, J., C. Wang, H. Shi, H.J. Qiu, S. Liu, D. Shi, X. Zhang, and L. Feng. 2011. Complete genome sequence of a Chinese virulent porcine epidemic diarrhea virus strain. *Journal of Virology* 85: 11538–11539. <https://doi.org/10.1128/JVI.06024-11>.
- Chen, J., X. Liu, D. Shi, H. Shi, X. Zhang, and L. Feng. 2012. Complete genome sequence of a porcine epidemic diarrhea virus variant. *Journal of Virology* 86: 3408. <https://doi.org/10.1128/JVI.07150-11>.
- Chen, J., X. Liu, H. Lang, Z. Wang, D. Shi, H. Shi, X. Zhang, and L. Feng. 2013. Genetic variation of nucleocapsid genes of porcine epidemic diarrhea virus field strains in China. *Archives of Virology* 158: 1397–1401. <https://doi.org/10.1007/s00705-013-1608-8>.
- Chen, Q., P.C. Gauger, M.R. Stafne, J.T. Thomas, D.M. Madson, H. Huang, Y. Zheng, G. Li, and J. Zhang. 2016a. Pathogenesis comparison between the United States porcine epidemic diarrhea virus prototype and S-INDEL-variant strains in conventional neonatal piglets. *Journal of General Virology* 97: 1107–1121. <https://doi.org/10.1099/jgv.0.000419>.
- Chen, Q., J.T. Thomas, L.G. Gimenez-Lirola, J.M. Hardham, Q. Gao, P.F. Gerber, T. Opriessnig, Y. Zheng, G. Li, P.C. Gauger, et al. 2016b. Evaluation of serological cross-reactivity and cross-neutralization between the United States porcine epidemic diarrhea virus prototype and S-INDEL-variant strains. *BMC Veterinary Research* 12: 70. <https://doi.org/10.1186/s12917-016-0697-5>.
- Deng, F., G. Ye, Q. Liu, M.T. Navid, X. Zhong, Y. Li, C. Wan, S. Xiao, Q. He, Z.F. Fu, et al. 2016. Identification and comparison of receptor binding characteristics of the spike protein of two porcine epidemic diarrhea virus strains. *Viruses* 8: 55. <https://doi.org/10.3390/v8030055>.
- Ding, T., T. Cheng, X. Zhu, W. Xiao, S. Xia, L. Fang, P. Fang, and S. Xiao. 2023. Exosomes mediate the antibody-resistant intercellular transmission of porcine epidemic diarrhea virus. *Veterinary Microbiology* 284: 109834. <https://doi.org/10.1016/j.vetmic.2023.109834>.
- Dong, N., L. Fang, H. Yang, H. Liu, T. Du, P. Fang, D. Wang, H. Chen, and S. Xiao. 2016. Isolation, genomic characterization, and pathogenicity of a Chinese porcine deltacoronavirus strain CHN-HN-2014. *Veterinary Microbiology* 196: 98–106. <https://doi.org/10.1016/j.vetmic.2016.10.022>.
- Gallien, S., A. Moro, G. Lediguerher, V. Catinot, F. Paboeuf, L. Bigault, P.C. Gauger, N. Pozzi, M. Berri, E. Authie, et al. 2019. Limited shedding of an S-INDEL strain of porcine epidemic diarrhea virus (PEDV) in semen and questions regarding the infectivity of the detected virus. *Veterinary Microbiology* 228: 20–25. <https://doi.org/10.1016/j.vetmic.2018.09.025>.
- Goede, D., M.P. Murtaugh, J. Nerem, P. Yeske, K. Rossow, and R. Morrison. 2015. Previous infection of sows with a "mild" strain of porcine epidemic diarrhea virus confers protection against infection with a "severe" strain. *Veterinary Microbiology* 176: 161–164. <https://doi.org/10.1016/j.vetmic.2014.12.019>.
- Grasland, B., L. Bigault, C. Bernard, H. Quenault, O. Toulouse, C. Fablet, N. Rose, F. Touzain, and Y. Blanchard. 2015. Complete genome sequence of a porcine epidemic diarrhea s gene indel strain isolated in france in December 2014. *Genome Announcements* 3: e00535-e615. <https://doi.org/10.1128/genomeA.00535-15>.
- Guo, J., L. Fang, X. Ye, J. Chen, S. Xu, X. Zhu, Y. Miao, D. Wang, and S. Xiao. 2019. Evolutionary and genotypic of global porcine epidemic diarrhea virus strains. *Transboundary and Emerging Diseases* 66: 111–118. <https://doi.org/10.1111/tbed.12991>.
- Have, P., V. Moving, V. Svansson, Å. Uttenthal, and B. Bloch. 1992. Coronavirus infection in mink (*Mustela vison*). Serological evidence of infection with a coronavirus related to transmissible gastroenteritis virus and porcine epidemic diarrhea virus. *Veterinary Microbiology* 31: 1–10. [https://doi.org/10.1016/0378-1135\(92\)90135-g](https://doi.org/10.1016/0378-1135(92)90135-g).
- Hou, Y., C.M. Lin, M. Yokoyama, B.L. Yount, D. Marthaler, A.L. Douglas, S. Ghimire, Y. Qin, R.S. Baric, L.J. Saif, et al. 2017. Deletion of a 197-amino-acid region in the N-terminal domain of spike protein attenuates porcine epidemic diarrhea virus in piglets. *Journal of Virology* 91: e00227-e317. <https://doi.org/10.1128/JVI.00227-17>.
- Katoh, K., and D.M. Standley. 2013. MAFFT multiple sequence alignment software version 7: Improvements in performance and usability. *Molecular Biology and Evolution* 30: 772–780. <https://doi.org/10.1093/molbev/mst010>.
- Kim, D.M., S.H. Moon, S.C. Kim, T.G. Lee, H.S. Cho, and D. Tark. 2024. Genome characterization of a Korean isolate of porcine epidemic diarrhea virus. *Microbiol Resour Announc* 13: e0011823. <https://doi.org/10.1128/mra.00118-23>.
- Kosakovsky Pond, S.L., and S.D. Frost. 2005. Not so different after all: A comparison of methods for detecting amino acid sites under selection. *Molecular Biology and Evolution* 22: 1208–1222. <https://doi.org/10.1093/molbev/msi105>.
- Lee, S., and C. Lee. 2014. Outbreak-related porcine epidemic diarrhea virus strains similar to US strains, South Korea, 2013. *Emerging Infectious Diseases* 20: 1223–1226. <https://doi.org/10.3201/eid2007.140294>.
- Li, M., Y. Zhang, Y. Fang, S. Xiao, P. Fang, and L. Fang. 2023. Construction and immunogenicity of a trypsin-independent porcine epidemic diarrhea virus variant. *Frontiers in Immunology* 14: 1165606. <https://doi.org/10.3389/fimmu.2023.1165606>.
- Li, W., F.J.M. van Kuppeveld, Q. He, P.J.M. Rottier, and B.J. Bosch. 2016. Cellular entry of the porcine epidemic diarrhea virus. *Virus Research* 226: 117–127. <https://doi.org/10.1016/j.virusres.2016.05.031>.
- Lin, C.M., T. Annamalai, X. Liu, X. Gao, Z. Lu, M. El-Tholoth, H. Hu, L.J. Saif, and Q. Wang. 2015a. Experimental infection of a US spike-insertion deletion porcine epidemic diarrhea virus in conventional nursing piglets and cross-protection to the original US PEDV infection. *Veterinary Research* 46: 134. <https://doi.org/10.1186/s13567-015-0278-9>.
- Lin, C.M., X. Gao, T. Oka, A.N. Vlasova, M.A. Esselli, Q. Wang, and L.J. Saif. 2015b. Antigenic relationships among porcine epidemic diarrhea virus and transmissible gastroenteritis virus strains. *Journal of Virology* 89: 3332–3342. <https://doi.org/10.1128/JVI.03196-14>.

- Lin, C.M., L.J. Saif, D. Marthaler, and Q. Wang. 2016. Evolution, antigenicity and pathogenicity of global porcine epidemic diarrhea virus strains. *Virus Research* 226: 20–39. <https://doi.org/10.1016/j.virusres.2016.05.023>.
- Lu, M., W. Wan, Y. Li, H. Li, B. Sun, K. Yu, J. Zhao, G. Franzo, and S. Su. 2023. Codon usage bias analysis of the spike protein of human coronavirus 229E and its host adaptability. *International Journal of Biological Macromolecules* 253: 127319. <https://doi.org/10.1016/j.ijbiomac.2023.127319>.
- Mesquita, J.R., R. Hakze-van der Honing, A. Almeida, M. Lourenco, W.H. van der Poel, and M.S. Nascimento. 2015. Outbreak of porcine epidemic diarrhea virus in Portugal, 2015. *Transboundary and Emerging Diseases* 62: 586–588. <https://doi.org/10.1111/tbed.12409>.
- Murrell, B., J.O. Wertheim, S. Moola, T. Weighill, K. Scheffler, and S.L. Kosakovsky Pond. 2012. Detecting individual sites subject to episodic diversifying selection. *PLoS Genetics* 8: e1002764. <https://doi.org/10.1371/journal.pgen.1002764>.
- Murrell, B., S. Moola, A. Mabona, T. Weighill, D. Sheward, S.L. Kosakovsky Pond, and K. Scheffler. 2013. FUBAR: A fast, unconstrained bayesian approximation for inferring selection. *Molecular Biology and Evolution* 30: 1196–1205. <https://doi.org/10.1093/molbev/mst030>.
- Nemeth, B., A. Fasseeh, A. Molnar, I. Bitter, M. Horvath, K. Koczian, A. Gotze, and B. Nagy. 2018. A systematic review of health economic models and utility estimation methods in schizophrenia. *Expert Review of Pharmacoeconomics & Outcomes Research* 18: 267–275. <https://doi.org/10.1080/14737167.2018.1430571>.
- Nguyen, L.T., H.A. Schmidt, A. von Haeseler, and B.Q. Minh. 2015. IQ-TREE: A fast and effective stochastic algorithm for estimating maximum-likelihood phylogenies. *Molecular Biology and Evolution* 32: 268–274. <https://doi.org/10.1093/molbev/msu300>.
- Ojkic, D., M. Hazlett, J. Fairles, A. Marom, D. Slavic, G. Maxie, S. Alexandersen, J. Pasick, J. Alsop, and S. Burlatschenko. 2015. The first case of porcine epidemic diarrhea in Canada. *Canadian Veterinary Journal* 56: 149–152. <https://doi.org/10.4141/cjas2014-117>.
- Rambaut, A., A.J. Drummond, D. Xie, G. Baele, and M.A. Suchard. 2018. Posterior summarization in Bayesian phylogenetics using Tracer 1.7. *Systematic Biology* 67: 901–904. <https://doi.org/10.1093/sysbio/syy032>.
- Rattanapisit, K., C.J.I. Bulaon, N. Khorattanakulchai, B. Shanmugaraj, K. Wangkanont, and W. Phoolcharoen. 2021. Plant-produced SARS-CoV-2 receptor binding domain (RBD) variants showed differential binding efficiency with anti-spike specific monoclonal antibodies. *PLoS One* 16: e0253574. <https://doi.org/10.1371/journal.pone.0253574>.
- Sato, T., N. Takeyama, A. Katsumata, K. Tuchiya, T. Kodama, and K. Kusanagi. 2011. Mutations in the spike gene of porcine epidemic diarrhea virus associated with growth adaptation in vitro and attenuation of virulence in vivo. *Virus Genes* 43: 72–78. <https://doi.org/10.1007/s11262-011-0617-5>.
- Schumacher, L., Q. Chen, L. Fredericks, P. Gauger, M. Bandrick, M. Keith, L. Gimenez-Lirola, D. Magstadt, W. Yim-Im, M. Welch, et al. 2022. Evaluation of the efficacy of an S-INDEL PEDV strain administered to pregnant gilts against a virulent non-S-INDEL PEDV challenge in newborn piglets. *Viruses* 14: 1801. <https://doi.org/10.3390/v14081801>.
- Smith, M.D., J.O. Wertheim, S. Weaver, B. Murrell, K. Scheffler, and S.L. Kosakovsky Pond. 2015. Less is more: An adaptive branch-site random effects model for efficient detection of episodic diversifying selection. *Molecular Biology and Evolution* 32: 1342–1353. <https://doi.org/10.1093/molbev/msv022>.
- Song, D., and B. Park. 2012. Porcine epidemic diarrhea virus: A comprehensive review of molecular epidemiology, diagnosis, and vaccines. *Virus Genes* 44: 167–175. <https://doi.org/10.1007/s11262-012-0713-1>.
- Stadler, J., S. Zoels, R. Fux, D. Hanke, A. Pohlmann, S. Blome, H. Weissenböck, C. Weissenbacher-Lang, M. Ritzmann, and A. Ladinig. 2015. Emergence of porcine epidemic diarrhea virus in southern Germany. *BMC Veterinary Research* 11: 142. <https://doi.org/10.1186/s12917-015-0454-1>.
- Sun, M., J. Ma, Y. Wang, M. Wang, W. Song, W. Zhang, C. Lu, and H. Yao. 2015. Genomic and epidemiological characteristics provide new insights into the phylogeographical and spatiotemporal spread of porcine epidemic diarrhea virus in Asia. *Journal of Clinical Microbiology* 53: 1484–1492. <https://doi.org/10.1128/JCM.02898-14>.
- Suzuki, T., T. Shibahara, R. Yamaguchi, K. Nakade, T. Yamamoto, A. Miyazaki, and S. Ohashi. 2016. Pig epidemic diarrhea virus S gene variant with a large deletion nonlethal to colostrum-deprived newborn piglets. *Journal of General Virology* 97: 1823–1828. <https://doi.org/10.1099/jgv.0.000513>.
- Suzuki, T., Y. Terada, L. Enjuanes, S. Ohashi, and W. Kamitani. 2018. S1 Subunit of spike protein from a current highly virulent porcine epidemic diarrhea virus is an important determinant of virulence in piglets. *Viruses* 10: 467. <https://doi.org/10.3390/v10090467>.
- Van Diep, N., J. Norimine, M. Sueyoshi, N.T. Lan, T. Hirai, and R. Yamaguchi. 2015. US-like isolates of porcine epidemic diarrhea virus from Japanese outbreaks between 2013 and 2014. *Springerplus* 4: 756. <https://doi.org/10.1186/s40064-015-1552-z>.
- Vlasova, A.N., D. Marthaler, Q. Wang, M.R. Culhane, K.D. Rossow, A. Rovira, J. Collins, and L.J. Saif. 2014. Distinct characteristics and complex evolution of PEDV strains, North America, May 2013–February 2014. *Emerging Infectious Diseases* 20: 1620–1628. <https://doi.org/10.3201/eid2010.140491>.
- Wang, L., B. Byrum, and Y. Zhang. 2014. New variant of porcine epidemic diarrhea virus, United States, 2014. *Emerging Infectious Diseases* 20: 917–919. <https://doi.org/10.3201/eid2005.140195>.
- Wanitchang, A., J. Saenboonrueng, C. Kaewborisuth, K. Srisutthisamphan, and A. Jongkaewwattana. 2019. A single V672F substitution in the spike protein of field-isolated PEDV promotes cell-cell fusion and replication in VeroE6 cells. *Viruses* 11: 282. <https://doi.org/10.3390/v11030282>.
- Wood, E.N. 1977. An apparently new syndrome of porcine epidemic diarrhea. *The Veterinary Record* 100: 243–244. <https://doi.org/10.1136/vr.100.12.243>.
- Zhao, Z., B.A. Sokhansanj, C. Malhotra, K. Zheng, and G.L. Rosen. 2020. Genetic grouping of SARS-CoV-2 coronavirus sequences using informative subtype markers for pandemic spread visualization. *PLoS Computational Biology* 16: e1008269. <https://doi.org/10.1371/journal.pcbi.1008269>.

Publisher's Note

Springer Nature remains neutral with regard to jurisdictional claims in published maps and institutional affiliations.